Wide-Area Damping Controller of FACTS Devices for Inter-Area Oscillations Considering Communication Time Delays

Wei Yao[1,2], L. Jiang[2], Jinyu Wen[1], Q. H. Wu[2], Shijie Cheng[1]

[1]State Key Laboratory of Advanced Electromagnetic Engineering and Technology, Huazhong University of Science and Technology, Wuhan, 430074, China.
[2]Department of Electrical Engineering and Electronics, The University of Liverpool, Liverpool, L69 3GJ, UK.

Abstract: The usage of remote signal obtained from a wide-area measurement system (WAMS) introduces time delays to a wide-area damping controller (WADC), which would degrade system damping and even cause system instability. The time delay margin is defined as the maximum time delay under which a closed-loop system can retain stable. In this paper, the delay margin is introduced as an additional performance index for the synthesis of classical WADCs for flexible AC transmission systems (FACTS) devices to damp inter-area oscillations. The proposed approach includes three parts: a geometric measure approach for selecting feedback remote signals, a residue method for designing phase compensation parameters, and a Lyapunov stability criterion and linear matrix inequalities (LMI) for calculating the delay margin and determining the gain of the WADC based on a trade-off between damping performance and delay margin. Three case studies are undertaken based on a four-machine two-area power system for demonstrating the design principle of the proposed approach, a New England 10-machine 39-bus power system and a 16-machine 68-bus power system for verifying the feasibility on larger and more complex power systems. The simulation results verify the effectiveness of the proposed approach on providing a balance between the delay margin and the damping performance.

Keywords: Wide-area damping controller, FACTS devices, inter-area oscillations, geometric observability, time delays, delay margin.

1. Introduction

Damping of inter-area low frequency oscillations is one of the main concerns for improving power system stability as those inter-area oscillations would reduce the reserve margin of the transmission capacity between areas of power grids [1]. The inter-area low frequency oscillations can be suppressed by installing power system stabilizers (PSSs) which provide supplementary control action through the excitation system of generators [2]; or an alternative by adding supplementary damping controllers to flexible AC transmission systems (FACTS) devices which are flexible to be installed at the key corridors of the grid [3]- [5] and thus can provide much better damping performance than PSSs [6]. These damping controllers conventionally use the local signals as feedback inputs have limitation for providing damping for some inter-area modes due to the lack of the observability of the inter-area mode from the local signals [1], though some specially designed controllers, such as self-tuning and robust controller, can still provide enough damping for some special inter-area oscillation modes [35].

With the development of the wide-area measurement system (WAMS), remote signals have become available as the feedback signals to design wide-area damping controllers (WADC) for FACTS devices [36]. The availability of remote signals can overcome the aforementioned shortcoming of lacking observability and provide flexibility to damp a special critical inter-area oscillation mode of power systems [1], [7]- [14]. Various control techniques have been used to the design/synthesis of WADC, such as classical lead-lag phase compensation based control [1], robust control [9]- [11], adaptive control [12], model predictive control [13], and neural network based optimal control [14].

On the other hand, although WADCs provide a great potential to improve the damping of inter-area oscillation, the usage of remote signals also introduce a new challenge into the design/synthesis of WADC, i.e., time delays caused by the usage of communication networks to transfer the remote signal will degrade the damping performance or may even cause instability of the closed-loop system [15, 18]. Those delays can typically vary from tens to several hundred milliseconds, depending on the distance, communication network, and protocol of transmission [16]- [17]. Moreover, calculation time of control law and faults of communication networks can also be converted into equivalent time delays [26]. However, most of these controllers mentioned above have not considered the influence of time delays introduced by the WAMS at the design stage.

Design of WADCs considering time delays have been addressed, such as applying nonlinear bang-bang control method to deal with time delays [37], designing robust controller to handle the time delay as a part of the system uncertainties [19]- [23], and compensating the time delays by designing a delay estimator [24]- [25]. On the other hand, delay-dependent stability analysis of WADC is investigated by calculating the maximal time delay (defined as delay margins) under which a power system equipped with a WADC can retain stable [26]. In [18, 27], delay-dependent stability analysis of load frequency control scheme and design of a robust load frequency controller by using delay margin as a new performance index are reported, respectively.

This paper proposes a systematic approach to design a WADC by introducing the delay margin as an additional performance index and combining it with conventional design techniques to deal with communication delays, and apply it for design a WADC for FACTS devices in a multi-machine power system. The proposed approach consists of three steps, i.e., modal analysis and selection of feedback signals based on the geometric measures method [28, 29], design of the phase compensation part based on the residue method [1], and determination of controller gain based on trade-off between delay margin and damping performance. Case studies are undertaken on a four-machine two-area power system, a New England 10-machine 39-bus power system, and a 16-machine 68-bus power system, respectively. The effectiveness of the proposed WADC is verified by simulation studies based on the detailed model.

This paper extends the work reported in [26] and its main contributions are summarized as follows:

- This paper concerns the design of a WADC for power system considering communication delays and proposes a systematic design approach for design of WADC by introducing the delay margin as an additional performance index into traditional control methods, while [26] mainly focuses on delay-dependent stability analysis of a power system equipped with a WADC.
- This paper generalizes the delay-dependent stability analysis method proposed in [26] and extends its application from analyzing WADC for generator exciter in [26] to a WADC for FACTS devices.
- Applications of the approach proposed have been verified on larger and complex power sys-

tems for designing WADC of SVC. Moreover, calculation method proposed in [26] has been verified by designing WADC for SVC in a small and two relatively larger and complex test power systems, while reference [26] only investigates the four-machine two-area power system.

2. Design of a Wide-area Damping Controller Considering Time Delay

Overall structure of a WADC designed for a FACTS device is illustrated in Fig. 1. The WADC is designed to damp a critical inter-area oscillation mode by providing supplementary damping control signal for the FACTS device. A classical lead-lag type WADC is considered. The time delays existing in remote signals obtained from the WAMS, other sources such as sampling measurements and control law calculation are simplified as one single delay d at the feedback loop and represented by a e^{-sd} block in Fig. 1.

As shown in Fig. 1, the transfer function of a classical WADC is:

$$H_{\mathrm{WADC}}(s) = K_{\mathrm{WADC}} \frac{T_w s}{1 + T_w s} \left(\frac{1 + T_1 s}{1 + T_2 s} \right)^m \tag{1}$$

where T_1 and T_2 are phase compensation parameters; T_w is the washout constant and usually chosen as $5 - 10$ seconds; K_{WADC} is the gain of the WADC; m is the number of the lead-lag block, usually, m is chosen to be 2.

The details of the proposed approach are described in the following subsections.

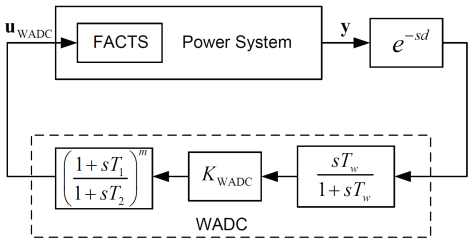

Fig. 1. *The structure of a WADC for a FACTS device*

2.1. Modal Analysis and Selection of Remote Feedback Signals

The dynamic model of power system is usually described by a set of differential-algebraic equations (DAEs). The whole power system excluding the WADC can be linearized at an equilibrium point as follows:

$$\begin{cases} \dot{\mathbf{x}}(t) = \mathbf{A}\mathbf{x}(t) + \mathbf{B}\mathbf{u}(t) \\ \mathbf{y}(t) = \mathbf{C}\mathbf{x}(t) \end{cases} \tag{2}$$

where $\mathbf{x} \in \mathbf{R}^{n\times 1}$, $\mathbf{y} \in \mathbf{R}^{q\times 1}$ and $\mathbf{u} \in \mathbf{R}^{p\times 1}$ are the vector of state variables, output variables and control variables, respectively; $\mathbf{A} \in \mathbf{R}^{n\times n}$ is the state matrix, $\mathbf{B} \in \mathbf{R}^{n\times p}$ the input matrix and $\mathbf{C} \in \mathbf{R}^{q\times n}$ the output matrix. Suppose matrix $\mathbf{A}$ has distinct eigenvalues $\lambda_k (k = 1, 2, ..., n)$ and the corresponding matrices of right and left eigenvectors, respectively, $\boldsymbol{\varphi}$ and $\boldsymbol{\psi}$.

Modal analysis of the linear model (2) is applied to find out the low frequency oscillation modes and then identify the critical inter-area mode. Modal observability have been used to select

a suitable feedback signal for WADC, such as residue measures [29] and geometric measures [10, 28]. As the geometric measures can evaluate the comparative strength of a signal and the performance of a controller against to a given mode, this paper adopts geometric measures to design the WADC [29].

The geometric measures of controllability $gm_{ci}(k)$ and observability $gm_{\mathrm{o}j}(k)$ associated with the k^{th} mode are

$$gm_{ci}(k) = \cos(\alpha(\boldsymbol{\psi}_k, \boldsymbol{b}_i)) = \frac{|\boldsymbol{b}_i^T \boldsymbol{\psi}_k|}{||\boldsymbol{\psi}_k||||\boldsymbol{b}_i||} \tag{3}$$

$$gm_{\mathrm{o}j}(k) = \cos(\theta(\boldsymbol{\varphi}_k, \boldsymbol{c}_j^T)) = \frac{|\boldsymbol{c}_j \boldsymbol{\varphi}_k|}{||\boldsymbol{\varphi}_k||||\boldsymbol{c}_j||} \tag{4}$$

where $\boldsymbol{b}_i$ the i^{th} column of input matrix $\mathbf{B}$ (corresponding to the i^{th} input) and $\mathbf{c}_j$ the j^{th} row of output matrix $\mathbf{C}$ (corresponding to the j^{th} output). $|\mathbf{z}|$ and $||\mathbf{z}||$ are the modulus and Euclidean norm of $\mathbf{z}$, respectively; $\alpha(\boldsymbol{\psi}_k, \boldsymbol{b}_i)$ is the geometrical angle between the input vector i and the k^{th} left eigenvector, while $\theta(\boldsymbol{\varphi}_k, \boldsymbol{c}_j^T)$ is the geometrical angle between the output vector j and the k^{th} right eigenvector.

Since every control-loop may have significant effect to several low frequency modes, it is recommended that the geometric observability measure should not be used as the only index for choosing wide-area control loop [38]. The joint controllability/observability measure (JCOM) is defined by

$$gm_{cok}(i, j) = gm_{ci}(k) gm_{oj}(k) \tag{5}$$

The selected wide-area control loop should have large JCOM to the concerned critical inter-area mode, while small JCOM to other modes so as to reduce interaction to other modes. Therefore, the remote signal with the relatively large JCOM to the critical inter-area mode and relatively small JCOM to other inter-area modes should be selected as the input feedback signal.

2.2. Design of Phase Compensation Part

To achieve the damping of one oscillation mode, the eigenvalue corresponding to that mode must be placed at the left-half of the complex plane. This can be done by using phase compensation method described in [1]. Assumption R_{kj} is the residue of the transfer function G_j with regard to the k-th mode, the amount of phase required compensation ϕ_k, with regard to the k^{th} mode, is given by:

$$\phi_k = \pi - \arg R_{kj} \tag{6}$$

Then the parameters of the lead-lag compensation part of WADC can be obtained by [30]:

$$\alpha = \frac{T_2}{T_1} = \frac{1 - \sin(\phi_k/m)}{1 + \sin(\phi_k/m)} \tag{7}$$

$$T_1 = \frac{1}{2\pi f_k \sqrt{\alpha}}, T_2 = \alpha T_1 \tag{8}$$

where f_k is the frequency of the k^{th} mode.

The value of the gain K_{WADC} influences not only the damping ratio of the k^{th} mode concerned but also the delay margin of the whole closed-loop system. Thus, the gain K_{WADC} should be determined by considering both the damping performance and the delay margin.

2.3. Determination of Controller Gain

The delay-dependent criterion proposed in [26] is used to determine the delay margin of power system embedded with a WADC and then the delay margin obtained will be used as a new performance index to design the WADC. The proposed approach includes the following steps: reducing the order of the power system excluding the controller, building up a closed-loop time-delay model, calculating delay margin of the closed-loop system and damp ratio of the concerned critical inter-area mode, and finally obtain the controller gain based on a trade-off between damping performance and delay margin. By satisfying a given delay margin requirement, the gain of the WADC should be chosen as larger as possible in order to improve the damping performance of the closed-loop power system.

Based on the Schur model reduction method [31], the reduced-order system of the open-loop power system can be found as follows:

$$\begin{cases} \dot{\mathbf{x}}_1(t) &= \mathbf{A}_1\mathbf{x}_1(t) + \mathbf{B}_1 u(t) \\ y(t) &= \mathbf{C}_1\mathbf{x}_1(t) \end{cases} \tag{9}$$

where $\mathbf{x}_1$ is the vector of state variables, $\mathbf{A}_1$ the state matrix, $\mathbf{B}_1$ the input matrix and $\mathbf{C}_1$ the output matrix of the control system of the reduced-order power system.

The transfer function model of WADC shown in (1) should be converted to state-space model as:

$$\begin{cases} \dot{\mathbf{x}}_2(t) &= \mathbf{A}_2\mathbf{x}_2(t) + \mathbf{B}_2 u_2(t) \\ y_2(t) &= \mathbf{C}_2\mathbf{x}_2(t) + D_2 u_2(t) \end{cases} \tag{10}$$

where $\mathbf{x}_2$ is the vector of state variables of the controller, $\mathbf{y}_2$ the vector of defined output variables, u_2 the vector of control variables, $\mathbf{A}_2$ the state matrix, $\mathbf{B}_2$ the input matrix and $\mathbf{C}_2$ the output matrix of the control system.

Thus, the model of the closed-loop power system considering time delay is obtained as:

$$\dot{\mathbf{x}}_{\mathrm{c}}(t) = \mathbf{A}_{\mathrm{c}}\mathbf{x}_{\mathrm{c}}(t) + \mathbf{A}_{\mathrm{d}}\mathbf{x}_{\mathrm{c}}(t - d(t)) \tag{11}$$

where $\mathbf{x}_{\mathrm{c}} = [\mathbf{x}_1, \mathbf{x}_2]^T$, and
$\mathbf{A}_{\mathrm{c}} = \begin{bmatrix} \mathbf{A}_1 & \mathbf{B}_1\mathbf{C}_2 \\ 0 & \mathbf{A}_2 \end{bmatrix}$, $\mathbf{A}_{\mathrm{d}} = \begin{bmatrix} \mathbf{B}_1 D_2 \mathbf{C}_1 & 0 \\ \mathbf{B}_2\mathbf{C}_1 & 0 \end{bmatrix}$.

In a delay-dependent system, asymptotic stability holds for $d < \tau_d$, where d denotes the time delay and τ_d is the delay margin, and the system is unstable for $d > \tau_d$. The delay margin τ_d is one of the critical parameters for evaluating the stability of the delay-dependent system. Throughout this paper, the constant time delay is denoted as d and the time-varying delay is denoted as $d(t)$, which is a continuous function of time and satisfies:

$$0 \le d(t) \le \tau, \quad |\dot{d}(t)| \le \mu \le 1 \tag{12}$$

where τ and μ are upper bounds of time delay and its rate, respectively. For a constant time delay, $\mu = 0$; $d(t) = d = \tau$. For a time-varying delay, $\mu \neq 0$; τ and μ are the upper bounds of the time delay and its rate, respectively.

The free-weighting matrices based delay-dependent stability criterion proposed in [26] will be applied to calculate the delay margin of the closed-loop power system in this paper. This method can deal with a linear system with constant and time-varying delays, and is a Lyapunov theory based indirect method and one of the methods with least conservativeness to calculate the delay

margin. The problem of calculating the delay margin of (11) can be converted into a standard generalized eigenvalue minimization problem by using this method and then the delay margin can be found by using LMI function $gevp$ provided in Matlab. The detailed description of this method is given in [26].

2.4. Summary of Steps of the Proposed Approach

Detailed steps of the proposed approach are summarized as follows:

Step 1: Building up a detailed model of the power system in MATLAB/Simulink and obtaining linear state-space model of the power system excluding the WADC at a chosen operating point by using Linear Analysis Toolbox provided in MATLAB.

Step 2: Carrying out modal analysis to find the frequencies and damping ratios of all low-frequency oscillation modes and identifying the critical inter-area mode.

Step 3: Selecting the feedback signal of the WADC based on the joint controllability/observability measure of candidate signals against to inter-area modes and choosing the one which has relative large geometric joint controllability/observability measure and less interactions to other inter-area modes.

Step 4: Determining the phase compensation parameters of the WADC by using the residue method.

Step 5: Obtaining the reduced-order model of the whole power system excluding the WADC using the Schur model reduction method [31], and obtaining reduced-order closed-loop system model including time-varying delay.

Step 6: Calculating the delay margins using the method described in [26] and damping ratios with regard to different gains K_{WADC}, respectively.

Step 7: Determining the gain of the WADC based on a trade-off between the damping performance and delay margin.

Step 8: Verifying the effectiveness of the designed WADC via simulation studies based on the original nonlinear detailed models.

3. Case Study I: Four-machine Two-area System

To illustrate the principle of the proposed approach firstly, a case study is undertaken on the four-machine two-area benchmark system, as shown in Fig. 2. The test system consists of two areas connected by two parallel 220km long tie-lines between bus $\#7$ and $\#9$. Each area consists of two generators, each is equipped with a standard governor, automatic voltage regulator (AVR) and IEEE ST1A type static exciter. The generator is represented by a 6^{th}-order sub-transient model. The load is modelled as constant impedance. Under nominal operating condition, approximately 400MW active power flows from Area 1 to Area 2. Both G1 and G3 are equipped with a PSS to damp the local mode oscillations. The detailed parameters of the system are given in [2].

Static VAR compensator (SVC), a common shunt compensation FACTS device widely used in power systems for improving voltage regulation, is chosen to be an example FACTS device [32]. As the voltage regulator of the SVC only provides small damping torque, it is necessary to augment a suitable WADC on the original control loop for improving the damping of inter-area oscillations [33]. The simulation studies are performed by using MATLAB/Simulink software.

SVC is installed to improve voltage profile of the grid via controlling its reactive power [32]. Therefore, the SVC should be generally installed at the bus which is closed to the load center

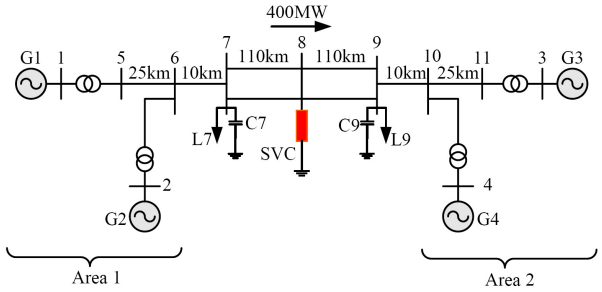

Fig. 2. *The four-machine two-area power system*

Table 1 Modal analysis results of the two-area system

Mode No.	Mode type	Damping ratio	Frequency (Hz)
1	Inter-area	0.0637	0.6216
2	Local	0.1884	1.1265
3	Local	0.1874	1.1676

and has low voltage level. In addition, the main tie-lines of the large-scale interconnected power systems are also considered as a suitable location to install SVC. Thus, for this test system, a SVC with capacity ± 200MVar is installed at bus #8.

3.1. Modal Analysis and Selection of Feedback Signals

Modal analysis results of the test system are given in Table 1. It can be found that Mode #1 is an inter-area mode where generators in Area 1 are oscillating against generators in Area 2. As it has a relatively small damping ratio 0.0637 and oscillation frequency 0.6216Hz, it is considered as the critical mode whose damping is desired to be improved by the WADC of the SVC.

The geometric observability measures associated with Mode #1 are calculated and then used to choose the feedback signal of the WADC, as shown in Table 2. For simplification, the geometric observability measure are normalized so that the largest element is equal to 1. As the rotor angle difference between G1 and G3 δ_{1-3} has largest geometric observability index, it is chosen as the remote feedback signal of the WADC.

Table 2 Geometric observability measure associated with Mode #1 of the two-area system

No.	Signal candidates	Geometric observability measure
1	δ_{1-3}	1.0000
2	I_{7-8}	0.9564
3	δ_{2-3}	0.9377
4	δ_{1-4}	0.9260
5	P_{7-8}	0.8688
6	I_{8-9}	0.8676
7	P_{8-9}	0.8633
8	δ_{2-4}	0.8633
9	I_{6-7}	0.6421
10	I_{9-10}	0.6421

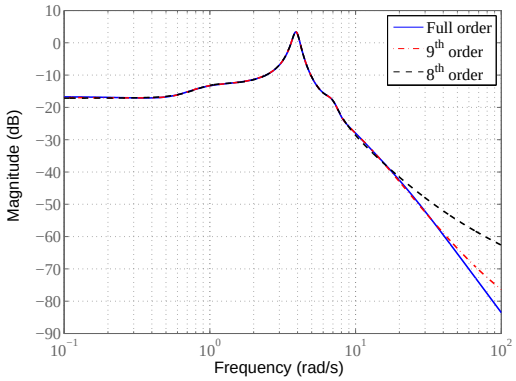

Fig. 3. *The frequency responses of the full-order and the reduced-order model of the two-area system*

3.2. Model Order Reduction

The open-loop system excluding the WADC is a 43^{th} order system. With choosing δ_{1-3} as output and u_{WADC} as input, the Schur balanced model reduction method is adopted [26]. The frequency responses of the reduced-order systems with different order and the full-order system are shown in Fig. 3. It can be found that when the model order is more than 8, the frequency response of the reduced-order system is very close to that of the full-order system over the frequency range from 0.1 rad/s to 50rad/s, which covers the concerned low-frequency oscillation range between 0.2 and 2.5Hz. Hence, the 9^{th}-order system is used for calculating the delay-margin of the closed-loop system.

3.3. Design of the WADC

The residue value obtained from the modal analysis of Mode #1 is $0.0072 + 0.3637i$. According to (7) and (8), the parameters of lead-lag compensation part of the WADC are given as: $T_w = 10$s, $T_1 = 0.6096$s, and $T_2 = 0.1075$s. The root locus of the closed-loop system without considering time delays is shown in Fig. 4. When K_{WADC} increases, the damping ratio of the critical inter-area Mode #1 increases. It can be concluded that the gain of the WADC K_{WADC} is the key parameter related with the damping performance of the Mode #1. To avoid an excessive interference of the main voltage regulator, the output of the WADC is limited by ± 0.1pu [2].

Based on the 9^{th}-order system model, the delay margin τ_d with respect to different sets of the gain K_{WADC} and the delay rate μ are calculated and summarized in Table 3. As same as in [26], we find that τ_d decreases with the increase of K_{WADC}. Moreover, for a fixed gain K_{WADC}, τ_d decreases with the increasing of μ. The relationship between damping ratio of Mode #1 and the gain of WADC is also given in Table 3, which shows that damping ratio ξ of the Mode #1 increases with the increasing of K_{WADC}. In summary, with the increase of the K_{WADC}, the damping ratio ξ increases while the delay margin τ_d decreases and vice versa. Therefore, the K_{WADC} can be tuned based on a trade-off between the damping performance and the delay margin.

Hence, when the delay margin of the closed-loop system satisfies a given practical requirement, the gain K_{WADC} should be chosen as greater as possible to enhance the damping of the Mode #1. From Table 3, when K_{WADC} increases from 0 to 0.7, the damping ratio of Mode #1 increases greatly from 0.0637 to 0.4020 (with the delay margin reduced from the infinite to 158.3ms). When

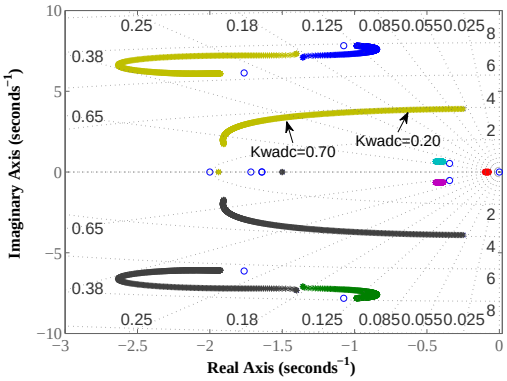

Fig. 4. *The root locus of the closed-loop two-area power system ($K_{\mathrm{WADC}} : 0 - 3.0$)*

Table 3 Delay margin and damping ratio of Mode #1 with respect to different K_{WADC} of Case I

	τ_d /ms [9^{th} order]			Mode #1	
K_{WADC}	$\mu = 0$	$\mu = 0.5$	$\mu = 0.9$	ξ	f (Hz)
0	—	—	—	0.0637	0.6216
0.12	505.5	503.4	503.4	0.1264	0.6164
0.15	451.9	451.9	451.9	0.1418	0.6145
0.20	399.8	399.8	399.8	0.1673	0.6108
0.30	338.9	329.7	302.4	0.2173	0.6012
0.50	248.6	194.8	194.2	0.3138	0.5741
0.70	158.3	152.8	152.8	0.4020	0.5365
1.00	123.9	111.7	102.8	0.5043	0.4734

K_{WADC} changes from 0.7 to 0.2, the damp ratio is reduced from 0.4020 to 0.1673 but with a significant increase of delay margin from 158.3 ms to 399.8 ms. As the time delay of the wide-area signal can typically vary from tens to several hundred milliseconds, the gain $K_{\mathrm{WADC}} = 0.2$ should be chosen for the WADC so that the closed-loop system has a large delay margin but still provides satisfactory damping performance.

3.4. Simulation Evaluation

Simulation studies are carried out based on the detailed model to verify the effectiveness of the proposed approach. The small disturbance applied for the case study is that the reference of G1 terminal voltage increases $+5\%$ at $t = 1$s.

The system responses of the WADC with $K_{\mathrm{WADC}} = 0.7$ and with $K_{\mathrm{WADC}} = 0.2$ under different time delays existing in the wide-area signal, are shown in Fig. 5 and Fig. 6, respectively. Without time delays, both WADCs can damp out the critical inter-area Mode #1 effectively and provide almost similar damping performances.

When the time delay is increased to 180ms, the WADC with gain $K_{\mathrm{WADC}} = 0.7$ cannot maintain system stability since time delay exceeds its delay margin 158.3ms. However, the WADC with gain $K_{\mathrm{WADC}} = 0.2$ can damp out the critical inter-area Mode #1 effectively even under a time delay as large as 300 ms. Moreover, when the time delay varies from 100ms to 300ms, the WADC with gain $K_{\mathrm{WADC}} = 0.2$ provides consistent damping performance, because it has a large delay

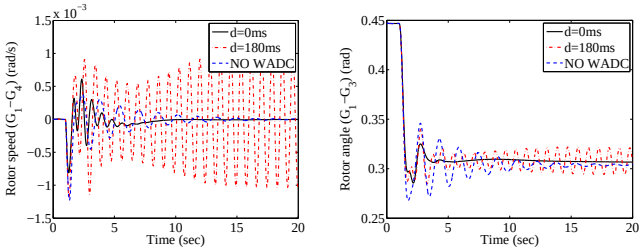

Fig. 5. *The responses of the two-area system with increasing $+5\%$ voltage reference of G1 under different time delays ($K_{\mathrm{WADC}} = 0.7$)*

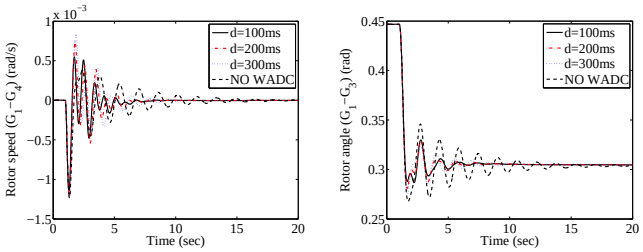

Fig. 6. *The responses of the two-area system with increasing $+5\%$ voltage reference of G1 under different time delays ($K_{\mathrm{WADC}} = 0.2$)*

margin 399.8 ms based on Table 3. This simulation results verify the gain $K_{\mathrm{WADC}} = 0.2$ should be determined for the WADC as the closed-loop system has a large delay margin and a satisfactory damp performance.

4. Case Study II: New England 10-machine 39-bus System

To investigate the feasibility of the proposed approach at a complex power system, a case study is undertaken based on the New England 10-machine 39-bus system, as shown in Fig. 7. This test system is a typical inter-connected system with poorly damped inter-area oscillation modes and has been widely used for studying the low frequency oscillation [10]. It consists of 10 generators, 39 buses, and 46 transmission lines. Each generator is modeled as a 4^{th}-order model and equipped with a IEEE DC1A excitation system, except generator G10 which is an equivalent infinite unit. The transmission system is modeled as a passive circuit and the loads are modeled as constant impedances. The mechanical power of each generator is assumed as constants for simplicity. The detailed parameters and operating conditions are given in [34]. The transmission lines between bus $\#15$ and $\#16$, bus $\#16$ and $\#17$ are the inter-area tie-lines which divide the entire system into two sub-systems. For this test system, since bus $\#16$ is the bus with low voltage profile, a ± 500Mvar SVC is installed at the bus $\#16$ to support the voltage profile.

4.1. Modal Analysis and Selection of Feedback Signals

After linearizing the model around a special operating point [34], modal analysis is carried out based on the linear model and the results obtained are shown in Table 4. It can be found that this system has several local and inter-area modes with damping ratios less than 0.1, in which Modes #1 to #3 are inter-area ones and Modes #4 to #9 are local ones. Although the damping ratios of Modes

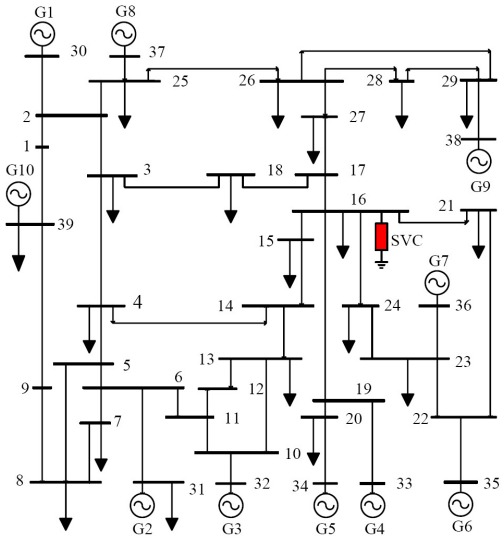

Fig. 7. *The New England 10-machine 39-bus power system*

Table 4 Modal analysis results of the New England system

Mode No.	Mode type	Damping ratio	Frequency (Hz)
1	Inter-area	0.0592	0.6093
2	Inter-area	0.0394	0.9310
3	Inter-area	0.0432	1.0390
4	Local	0.0445	1.1430
5	Local	0.0373	1.2735
6	Local	0.0378	1.4190
7	Local	0.0549	1.4658
8	Local	0.0442	1.5080
9	Local	0.0745	1.5110

#2 to #9 are small, they have relatively large frequency values. Thus the oscillation related with those modes will decay quickly and it is not necessary to provide supplementary damping control for those modes [10]. Therefore, the WADC of the SVC will be designed mainly for increasing the damping of the critical inter-area Mode #1, which has relatively small damping ratio 0.0592 and low oscillation frequency 0.6093Hz.

Table 5 and Fig. 8 show the JCOM of the wide-area signals to inter-area Mode #1, #2, #3. All JCOM values are normalized by using the largest JCOM as the based value. In Table 5, I_{i-j} represents the magnitude of current between bus #i and #j and P_{i-j} the active power between bus #i and #j. P_{3-18} is selected as the feedback signal for the WADC because it not only has the relatively large JCOM (at this case, it is the largest) to Mode #1 but also relatively small JCOM to Mode #2 and #3, among all candidates shown in Table 5.

4.2. Model Order Reduction

The model of the test system excluding WADC is 59^{th} order. With choosing the deviation of active power P_{3-18} as the output and u_{WADC} as the input, the Schur balanced model reduction method is

Table 5 Joint controllability/observability measure associated with Mode #1,#2,#3, of the New England system

		Joint controllability/observability measure		
No.	Signal candidates	Mode #1	Mode #2	Mode #3
1	P_{3-18}	1.0000	0.1450	0.0975
2	I_{17-18}	0.9844	0.4439	0.1532
3	P_{17-18}	0.9792	0.4429	0.1517
4	P_{5-8}	0.9543	0.1427	0.2333
5	P_{8-9}	0.9450	0.1417	0.2718
6	P_{9-39}	0.9439	0.1417	0.2717
7	P_{1-2}	0.9211	0.1920	0.1405
8	P_{1-39}	0.9211	0.1920	0.1405

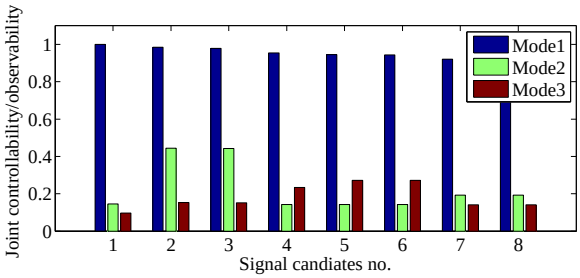

Fig. 8. *Joint controllability/observability measure associated with Mode #1-#3*

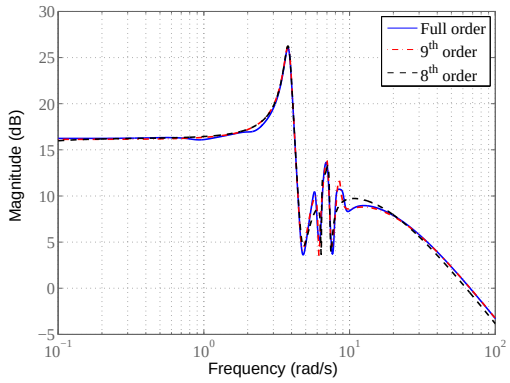

Fig. 9. *The frequency responses of the full-order and reduced-order model of the New England system*

applied. Comparing the frequency responses of the reduced-order with the full-order model shown in Fig. 9, the reduced model is determined as 9^{th}-order because it can provide similar frequency response with that of the full-order system over the concerned oscillation frequency range between 0.2 and 2.5Hz.

4.3. Design of WADC

For Mode #1, the residue value obtained from the linearized analysis is $0.4642 + 4.2678i$. According to (7) and (8), the parameters of lead-lag compensation part are given as: $T_w = 10$s,

Table 6 Delay margin and damping ratio of Mode #1 with respect to different K_{WADC} of the New England system

	τ_d /ms [9^{th} order]			Mode #1	
K_{WADC}	$\mu = 0$	$\mu = 0.5$	$\mu = 0.9$	ξ	f (Hz)
0	—	—	—	0.0592	0.6093
0.008	448.2	399.5	350.5	0.1213	0.6126
0.009	352.2	275.8	244.0	0.1290	0.6113
0.010	233.8	162.8	138.9	0.1366	0.6142
0.011	90.4	53.9	45.0	0.1441	0.6160
0.012	70.9	47.4	31.7	0.1515	0.6182
0.013	60.2	42.4	29.1	0.1586	0.6208
0.015	47.2	35.0	24.9	0.1718	0.6272
0.020	31.2	24.4	18.3	0.1932	0.6509

$T_1 = 0.6823$s, and $T_2 = 0.1000$s. The root locus of the closed-loop system without considering time delay is shown in Fig. 10. When K_{WADC} changes from 0 to 0.015, the damping ratio of the Mode #1 increases significantly from 0.0592 to 0.1718. To avoid the excessive interference of the main voltage regulator, the output of the WADC is limited by ± 0.1pu [2].

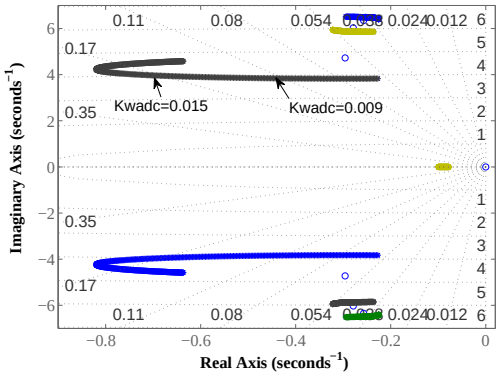

Fig. 10. *The root locus of the closed-loop New England power system ($K_{\mathrm{WADC}} : 0 - 0.05$)*

Based on the 9^{th}-order model, the delay margins τ_d with respect to different gains K_{WADC} and the delay rate μ are calculated and shown in Table 6. The damping ratio of Mode #1 under different gains are given in Table 6 as well. The relationship between gains and delay margins are as similar as as the simple case can be obtained.

As shown in Table 6, when K_{WADC} reduces from 0.015 to 0.009, the damping ratio reduces from 0.1718 to 0.1290, while the delay margin increases significantly from 47.2 ms to 352.2 ms. Therefore, the gain $K_{\mathrm{WADC}} = 0.009$ is determined for the WADC such that the closed-loop system has a large delay margin but still provides satisfactory damping performance.

4.4. Simulation Evaluation

Simulation studies are carried out based on detailed nonlinear model to verify the effectiveness of the designed WADC. A three-phase-to-ground fault occurs at the end terminal of line #3- #4 near bus #3 at $t = 0.5$s, followed by switching off the the faulty transmission line at $t = 0.6$s and switching on again at $t = 1.1$s. When there is no time delay existing in the wide-area signal, the

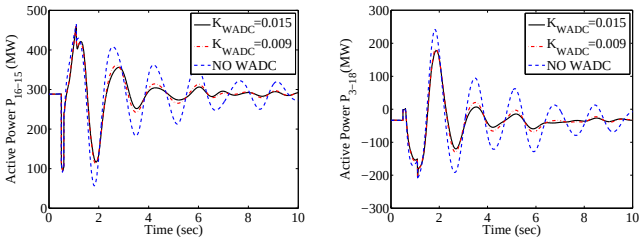

Fig. 11. *The responses of the New England power system to fault with different gains of the WADC*

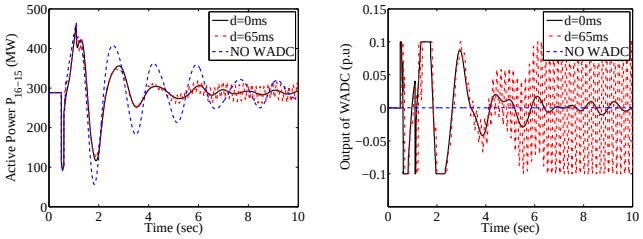

Fig. 12. *The responses of the New England power system to fault with different time delays* ($K_{\mathrm{WADC}} = 0.015$)

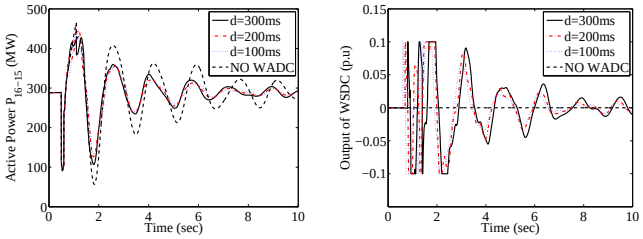

Fig. 13. *The responses of the New England power system to with different time delays* ($K_{\mathrm{WADC}} = 0.009$)

responses of the system are shown in Fig. 11. It is shown that the WADC can provide effective damping of inter-area oscillations and the WADC with gain $K_{\mathrm{WADC}} = 0.015$ provides slightly better damping performance than the WADC with gain $K_{\mathrm{WADC}} = 0.009$. This is also confirmed by the root locus of the closed-loop system shown in Fig. 10.

The system responses of the WADC with different time delays existing in the wide-area signal are shown in Fig. 12 and Fig. 13, respectively. When the time delay reaches to 65ms, the WADC with gain $K_{\mathrm{WADC}} = 0.015$ cannot maintain system stability as the time delay exceeds its delay margin 47.2ms, according to Table 6. However, the WADC with gain $K_{\mathrm{WADC}} = 0.009$ can damp out the critical inter-area Mode #1 effectively even with the time delay as large as 300 ms. Moreover, when the time delay varies from 100ms to 300ms, the WADC with gain $K_{\mathrm{WADC}} = 0.009$ provides almost similar damping performance. This is because the WADC with gain $K_{\mathrm{WADC}} = 0.009$ has a large delay margin 352.2 ms, as shown in Table 6. This simulation results verify the gain $K_{\mathrm{WADC}} = 0.009$ should be determined for the WADC as the closed-loop system has a large delay margin but still provides good damp performance.

The robustness of the proposed WADC against different operating conditions are verified by the following two scenarios. Scenario I is that the tripped faulty transmission line #3- #4 is not

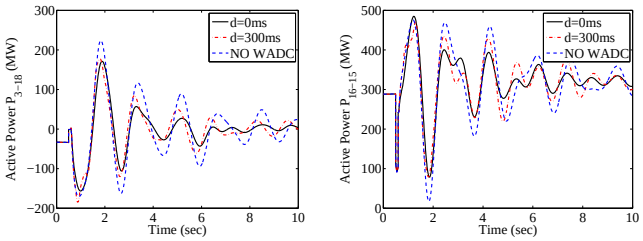

Fig. 14. *The responses of the New England power system to fault followed by outage of line #3-#4 ($K_{\mathrm{WADC}} = 0.009$)*

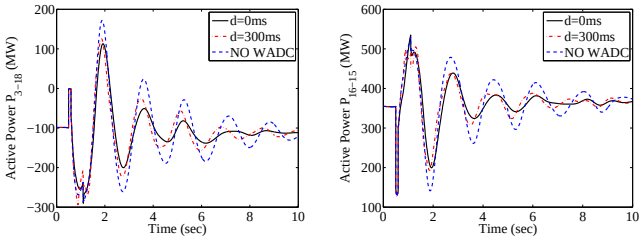

Fig. 15. *The responses of the New England power system to fault when active power of tie-line is* 670*MW ($K_{\mathrm{WADC}} = 0.009$)*

re-closed after the fault is cleared. Scenario II is that the total power flow of tie-lines (line #16-#15 and #16- #17) increases from 494MW to 670MW. Fig. 14 and Fig. 15 illustrate the system responses to Scenario I and Scenario II, respectively. It can be concluded that the proposed WADC can provide enough damping to the system and has satisfactory robustness against different operating conditions.

5. Case Study III: 16-machine 68-bus System

To further investigate the feasibility of the proposed approach in a more complex and realistic power system, design of WADC for SVC in a 16-machine 68-bus test system shown in Fig. 16 is given in this section. This system is a simplified New England and New York interconnected system and has been used to test the effectiveness of WADC in a relatively large power system [39, 40]. All generators are modeled via a 6th-order model, the governor dynamics are neglected while the IEEE ST1A excitation system is adopted for G1-G15, and all loads are represented as constant impedance. In addition, the PSS is equipped at G1-G12 to provide damping for local and inter-area oscillation modes. The detailed description of this test system including network data, parameters of generators and excitation systems are given in [39]. For this test system, a ± 600Mvar SVC is installed at the bus $\#51$ to maintain its voltage profile.

5.1. Modal Analysis and Selection of Feedback Signals

Modal analysis of this test system finds that it has four inter-area modes, as shown in Table 7. The Mode #1 and Mode #3 have enough damping ratios while the Mode #2 and Mode #4 are lightly damped. As frequency of Mode #4 is relatively higher than Model #2 and its related oscillation will not last more than 10 seconds, it does not required additional damping [40]. Thus, the main objec-

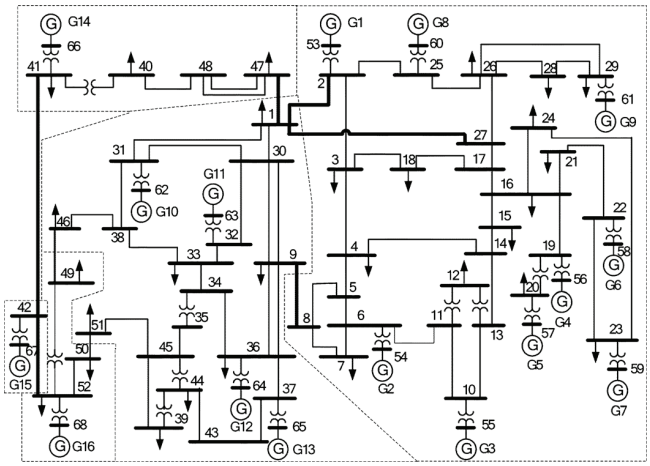

Fig. 16. *The 16-machine 68-bus power system*

Table 7 Modal analysis results of the 16-machine 68-bus system

Mode No.	Mode type	Damping ratio	Frequency (Hz)
1	Inter-area	0.1332	0.3791
2	Inter-area	0.0316	0.5365
3	Inter-area	0.1636	0.6585
4	Inter-area	0.0519	0.7957

tive is to design a WADC to provide damping to Mode #2, which has relatively lower frequency and the smallest damping ratio.

Fig. 17 and Table 8 show the JCOM of different wide-area signal candidates with respect to four inter-area modes. As shown in Table 8 and Fig. 17, the signal 1 (P_{46-38}) has the largest JCOM to the Mode #2, but also has relatively large JCOM to the Mode #1, which represents a potential modes interactions. The signal 5 (P_{68-52}) has smaller JCOM to Mode #2 than signal 1, but JCOM to all other modes are relatively small. Therefore, signal 5 P_{68-52} is selected as the feedback signal for the WADC because it not only has the relatively large JCOM among these candidates but also has smaller interaction to other three inter-area modes. Note that signal 2 and signal 6 represent current magnitude and are correlated closely to signal 1 and signal 5, respectively.

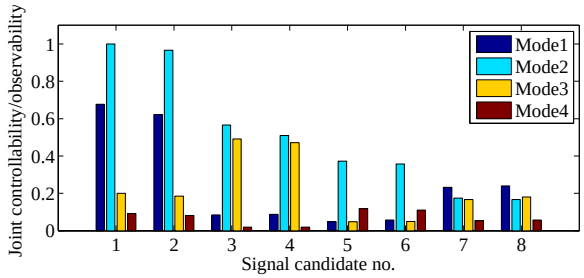

Fig. 17. *Joint controllability/observability measure associated with Mode #1-#4*

Table 8 Joint controllability/observability measure associated with Mode #1,#2,#3,#4, of the 16-machine 68-bus system

		Joint controllability/observability measure			
No.	Signal candidates	Mode #1	Mode #2	Mode #3	Mode #4
1	P_{46-38}	0.6769	1.0000	0.2000	0.0925
2	I_{46-38}	0.6227	0.9665	0.1844	0.0818
3	I_{1-31}	0.0851	0.5659	0.4907	0.0197
4	P_{1-31}	0.0882	0.5094	0.4711	0.0186
5	P_{68-52}	0.0483	0.3724	0.0475	0.1180
6	I_{68-52}	0.0576	0.3569	0.0488	0.1097
7	P_{31-30}	0.2319	0.1747	0.1670	0.0548
8	I_{31-30}	0.2402	0.1671	0.1806	0.0577

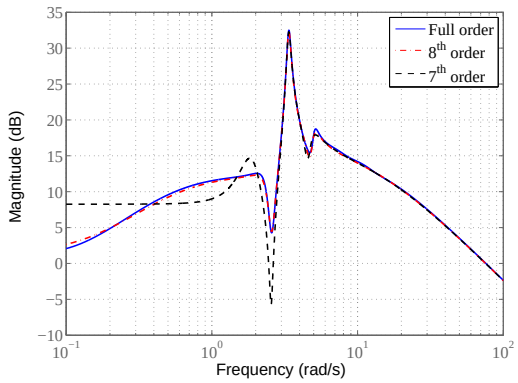

Fig. 18. *The frequency responses of the full-order and reduced-order model of the New England system*

5.2. Model Order Reduction

Via choosing the deviation of active power P_{68-52} as the output and u_{WADC} as the input, the Schur reduction method is applied to obtain a reduced-order model of the original 133^{th} order test system. Comparing the frequency responses of the reduced-order system with the full-order model over the concerned oscillation frequency range between 0.2 and 2.5Hz, as shown in Fig. 18, the order of the reduced model is determined as 8^{th}-order.

5.3. Design of WADC

For Mode #2, the residue value obtained from the linearized analysis is $2.0877 + 4.0014i$. According to (7) and (8), the parameters of lead-lag compensation part are obtained as: $T_w = 10$s, $T_1 = 0.5267$s, and $T_2 = 0.1671$s. The root locus of the closed-loop system without considering time delay is shown in Fig. 19. When K_{WADC} changes from 0 to 0.025, the damping ratio of the Mode #2 increases significantly from 0.0316 to 0.1643. It also can be found that the damping ratios of other three inter-area modes changed very little, which means the interaction of the WADC with other modes are trivial. This is because the JCOM of the control loop to these three inter-area modes are far smaller than that to Mode #2. Similarly, the output of the WADC is limited by ± 0.1pu.

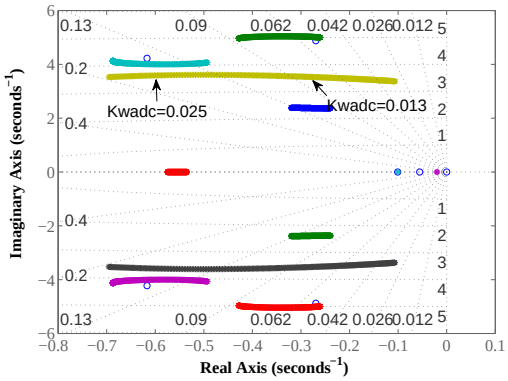

Fig. 19. *The root locus of the closed-loop 16-machine power system ($K_{\mathrm{WADC}} : 0 - 0.03$)*

Table 9 Delay margin and damping ratio of Mode #2 under different K_{WADC} of Case III

	τ_d /ms [8^{th} order]			Mode #2	
K_{WADC}	$\mu = 0$	$\mu = 0.5$	$\mu = 0.9$	ξ	f (Hz)
0	—	—	—	0.0316	0.5365
0.008	441.9	389.0	336.8	0.0559	0.5515
0.010	348.3	320.2	228.7	0.0636	0.5554
0.013	284.3	241.1	188.4	0.0768	0.5612
0.015	252.4	190.7	168.0	0.0869	0.5651
0.020	186.1	130.4	120.4	0.1198	0.5733
0.025	86.4	55.0	35.5	0.1643	0.5712
0.026	41.4	32.6	21.6	0.1722	0.5691

Based on the 8^{th}-order reduced model, the delay margins τ_d under different gains K_{WADC} and different delay rates μ are calculated and shown in Table 9. The damping ratio ξ and frequency f of Mode #2 under different gains K_{WADC} are also calculated and given in the last two columns of Table 9. Similar relationship between gains and delay margins can be obtained as Case Study I and II.

As shown in Table 9, when K_{WADC} reduces from 0.025 to 0.013, the damping ratio reduces from 0.1643 to 0.0768, while the delay margin increases significantly from 86.4 ms to 284.3 ms. Therefore, to provide a delay margin in the range between 250ms and 400ms, the gain $K_{\mathrm{WADC}} = 0.013$ should be chose with the cost of reduction of damping ratio from 0.1643 to 0.0768.

5.4. Simulation Evaluation

Simulation studies are carried out based on detailed nonlinear model to verify the effectiveness of the designed WADC. A three-phase-to-ground fault occurs at the end terminal of line #45- #51 near bus #45 at $t = 0.5$s and is cleared at $t = 0.6$s. When there is no time delay existing in the wide-area signal, the responses of the system are shown in Fig. 20. It is shown that the WADC can provide effective damping of inter-area oscillations and the WADC with gain $K_{\mathrm{WADC}} = 0.025$ provides slightly better damping performance than the WADC with gain $K_{\mathrm{WADC}} = 0.013$. This is also confirmed by the root locus of the closed-loop system shown in Fig. 19.

The system responses of the WADC under different time delays existing in the wide-area signal

are shown in Fig. 21 and Fig. 22, respectively. When the time delay reaches to 100ms, the WADC with gain $K_{\mathrm{WADC}} = 0.025$ cannot maintain system stability as the time delay exceeds its delay margin 86.4ms, according to Table 9. However, the WADC with gain $K_{\mathrm{WADC}} = 0.013$ can damp out the critical inter-area Mode #1 effectively even with the time delay as large as 250 ms. This is because the WADC with gain $K_{\mathrm{WADC}} = 0.013$ has a large delay margin 284.3 ms, as shown in Table 9. Therefore, the gain $K_{\mathrm{WADC}} = 0.013$ should be determined for the WADC as the closed-loop system has a large delay margin but still provides good damp performance.

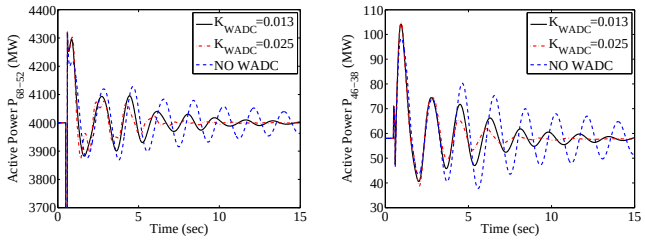

Fig. 20. *The responses of the 16-machine power system to fault without delay under different gains of the WADC*

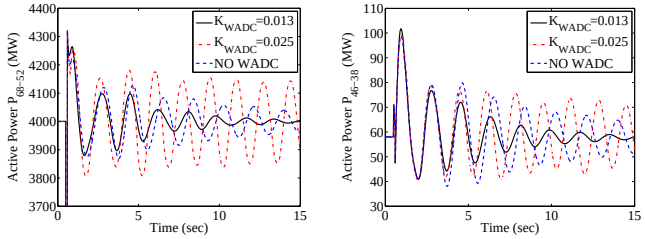

Fig. 21. *The responses of the 16-machine power system to fault with* 100*ms delay under different gains of the WADC*

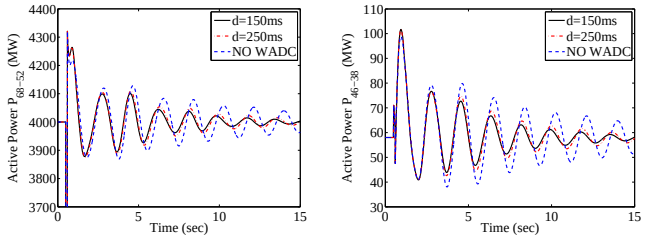

Fig. 22. *The responses of the 16-machine power system to fault under different time delays* ($K_{\mathrm{WADC}} = 0.013$)

6. Conclusion

This paper has presented a new approach for the synthesis of a wide-area damping controller for FACTS devices, considering the influence of communication time delays introduced by the usage of remote signals. The proposed approach introduces the delay margin as an additional

performance index and combines with the geometric measure method for selecting the feedback input signal and the residue method to design the phase compensation part of the WADC.

The delay margin is calculated by a Lyapunov stability criterion and linear matrix inequalities (LMI), based on the reduced-order model of the large-scale power system excluding the WADC. The gain of the WADC is a key parameter related with the delay margin and the damping performance: the increase of the gain of WADC will reduce the delay margin, while increase the damping ratio of the critical inter-area oscillation mode. Based on a tradeoff between the damping performance and the delay margin, the gain should be chose either to provide a satisfactory damping performance while with a larger delay margin, or as larger as possible to enhance the damping performance after the delay margin obtained from practical requirement is satisfied. The design of a classical lead-lag type WADC for SVC-type FACTS devices has been carried out by three case studies based on the four-machine two-area power system, the New England 10-machine 39-bus power system, and 16-machine 68-bus power system, respectively. Results of the case studies have verified the effectiveness of the proposed approach to achieve a compromise between damping performance and delay margin, and demonstrated the feasibility of its applications in a relatively large-scale power system.

Further studies will focus on coordinating design and tuning of WADCs for damping multiple inter-area oscillation modes by using results of the delay-dependent stability analysis of the power system with multiple time-varying delays.

7. References

[1] M. E. Aboul-Ela, A. A. Sallam, J. D. Mccalley, and A. A. Fouad, "Damping controller design for power system oscillations using global signals," *IEEE Trans. Power Syst.*, vol. 11, no. 2, pp. 767-773, May 1996.

[2] P. Kundur, *Power system stability and control*. New York: McGraw-Hill, 1994.

[3] R. V. de Oliveira, R. Kuiava, R. A. Ramos, and N. G. Bretas, "Automatic tuning method for the design of supplementary damping controllers for flexible alternating current transmission system devices," *IET Gener. Transm. Distrib.*, vol. 3, no. 10, pp. 919-929, Oct. 2009.

[4] M. M. Farsangi, H. Nezamabadi-pour, Y. H. Song, and K. Y. Lee, "Placement of SVCs and selection of stabilizing signals in power systems," *IEEE Trans. Power Syst.*, vol. 22, no. 3, pp. 1061 -1071, Aug. 2007.

[5] M. Zarghami, M. L. Crow, J. Sarangapani, Y. Liu, and S. Atcitty, "A novel approach to interarea oscillation damping by unified power flow controllers utilizing ultracapacitors," *IEEE Trans. Power Syst.*, vol. 25, no. 1, pp. 404-412, Feb. 2010.

[6] N. Mithulananthan, C. A. Canizares, J. Reeve, and G. J. Rogers, "Comparison of PSS, SVC, and STATCOM controllers for damping power system oscillations," *IEEE Trans. Power Syst.*, vol. 18, no. 2, pp. 786-792, May. 2003.

[7] V. Terzija, G. Valverde, D. Cai, P. Regulski, V. Madani, J. Fitch, S. Skok, M. Begovic, and A. Phadke, "Wide area monitoring, protection and control of future electric power networks", *Proc. IEEE*, vol. 99, no. 1, pp.80-93, Jan. 2011.

[8] Y. Chompoobutrgool, L. Vanfretti, and M. Ghandhai, "Survey on power system stabilizers control and their propective applications for power system damping using synchrophasor-based wide-area systems," *Eur. Trans. Electr. Power*, vol. 21, no.8, pp. 2098-2111, Nov. 2011.

[9] B. Chaudhuri and B. C. Pal, "Robust damping of multiple swing modes employing global stabilizing signals with a TCSC," *IEEE Trans. Power Syst.*, vol. 19, no. 1, pp. 499-506, Feb. 2004.

[10] Y. Zhang and A. Bose, "Design of wide-area damping controllers for interarea oscillations," *IEEE Trans. Power Syst.*, vol. 23, no. 3, pp. 1136-1143, Aug. 2008.

[11] Y. Li, C. Rehtanz, S. Ruberg, L. F. Luo, and Y. J. Cao, "Wide-area robust coordination approach of HVDC and FACTS controllers for damping multiple interarea oscillations," *IEEE Trans. Power Del.*, vol. 27, no. 3, pp. 1096-1105, Jul. 2012.

[12] N. R. Chaudhuri, D. Chakraborty, and B. Chaudhuri, "An architecture for FACTS controllers to deal with bandwidth-constrained communication," *IEEE Trans. Power Del.*, vol. 26, no. 1, pp. 188-196, Jan. 2011.

[13] E. Bijami, J. Askari, and M. M. Farsangi, "Design of stabilising signals for power system damping using generalised predictive control optimised by a new hybrid shuffled frog leaping algorithm," *IET Gener. Transm. Distrib.*, vol. 6, no. 10, pp. 1036-1045, Oct. 2012.

[14] S. Ray and G. K. Venayagamoorthy, "Wide-area signal-based optimal neurocontroller for a UPFC," *IEEE Trans. Power Del.*, vol. 23, no. 3, pp. 1597-1605, Jul. 2008.

[15] J. W. Stahlhut, T. J. Browne, G. T. Heydt, and V. Vittal, "Latency viewed as a stochastic process and its impact on wide area power system control signals," *IEEE Trans. Power Syst.*, vol. 23, no. 1, pp. 84-91, Feb. 2008.

[16] B. Naduvathuparambil, M. C. Valenti, and A. Feliachi, "Communication delays in wide area measurement systems," in *Proc. of the 34th Southeastern Symposium on System Theory*, pp. 118-122, Mar. 2002.

[17] K. Tomsovic, D. E. Bakken, V. Venkatasubramanian, and A. Bose, "Designing the next generation of real-time control, communication, and computations for large power systems", *Proc. IEEE*, vol. 93, no. 5, pp. 965-979, May 2005.

[18] L. Jiang, W. Yao, Q. H. Wu, J. Y. Wen, and S. J. Cheng. "Delay-dependent stability for load frequency control with constant and time-varying delays," *IEEE Trans. Power Syst.*, vol. 27, no. 2, pp. 932-941, May 2012.

[19] B. Chaudhuri, R. Majumder, and B. C. Pal, "Wide-area measurement-based stabilizing control of power system considering signal transmission delay," *IEEE Trans. Power Syst.*, vol. 19, no. 4, pp. 1971-1979, Nov. 2004.

[20] D. P. Ke, C. Y. Chung, and Y. Xue, "An eigenstructure-based performance index and its application to control design for damping inter-area oscillations in power systems," *IEEE Trans. Power Syst.*, vol. 26, no. 4, pp. 2371-2380, Nov. 2011.

[21] A. E. Leon, J. M. Manuel, A. Gomez-Exposito, and J. A. Solsona, "Hierarchical wide-area control of power systems including wind farms and FACTS for short-term frequency regulation," *IEEE Trans. Power Syst.*, vol. 27, no. 4, pp. 2084-2092, Nov. 2012.

[22] D. Dotta, A. S. Silva, and I. C. Decker, "Wide-area measurements-based two-level control design considering signal transmission delay," *IEEE Trans. Power Syst.*, vol. 24, no. 1, pp. 208-216, Feb. 2009.

[23] J. He, C. Lu, X. Wu, P. Li, and J. Wu, "Design and experiment of wide area HVDC supplementary damping controller considering time delay in China southern power grid," *IET Gener. Transm. Distrib.*, vol. 3, no. 1, pp. 17-25, Jan. 2009.

[24] R. Majumder, B. Chaudhuri, B. C. Pal, and Q. C. Zhong, "A unified Smith predictor approach for power system damping control design using remote signals," *IEEE Trans. Control Syst. Technol.*, vol. 13, no. 1, pp. 1063-1068, Nov. 2005.

[25] N. B. Chaudhuri, S. Ray, R. Majumder, and B. Chaudhuri, "A new approach to continuous latency compesation with adaptive phasor power oscillation damping controller (POD)," *IEEE Trans. Power Syst.*, vol. 25, no. 2, pp. 939-946, May 2010.

[26] W. Yao, L. Jiang, Q. H. Wu, J. Y. Wen, and S. J. Cheng. "Delay-dependent stability analysis of the power system with a wide-area damping controller embedded," *IEEE Trans. Power Syst.*, vol. 26, no. 1, pp. 233-240, Feb. 2011.

[27] C. K. Zhang, L. Jiang, Q. H. Wu, Y. He, and M. Wu. "Delay-dependent robust load frequency control for time delay power systems," *IEEE Trans. Power Syst.*, vol. 28, no. 3, pp. 2192-2201, Aug. 2013.

[28] A. M. A. Hamdan and A. M. Elabdalla, "Geometric measures of modal controllability and observability of power system models," *Electr. Power Syst. Res.*, vol. 15, no. 2, pp. 147-155, Oct. 1988.

[29] A. Heniche and I. Kamwa, "Assessment of two methods to select wide-area signals for power system damping control," *IEEE Trans. Power Syst.*, vol. 23, no. 2, pp. 572-581, May. 2008.

[30] Y. Chang and Z. Xu, "A novel SVC supplementary controller based on wide area signals," *Electr. Power Syst. Res.*, vol. 77, no. 2, pp. 1569-1574, Oct. 2007.

[31] G. Balas, R. Chiang, A. Packard, and M. Safonov, "Robust Control Toolbox Users Guide,". Natick, MA: MathWorks, 2005.

[32] X. P. Zhang, C. Rehtanz, and B. Pal, *Flexible AC transmission systems: modeling and control*. Berlin: Springer, 2012.

[33] P. K. Dash, S. Mishra, and A. C. Liew, "Fuzzy-logic-based VAR stabiliser for power system control," *IEE Proc. Gener. Transm. Distrib.*, vol. 142, no. 6, pp. 618-624, Nov. 1995.

[34] M. A. Pai, *Energy function analysis for power system stability*. Boston, MA: Kluwer, 1989.

[35] I. Kamwa, G. Trudel, and L. Gerin-Lajoie, "Robust design and coordination of multiple damping controllers using nonlinear constrained optimization," *IEEE Trans. Power Syst.*, vol. 15, no. 3, pp. 1084-1092, Aug. 2000.

[36] I. Kamwa, R.Grondin, and Y. Hebert, "Wide-area measurement based stabilizing control of large power systems - a decentralized/hierarchical approach," *IEEE Trans. Power Syst.*, vol. 16, no. 1, pp. 136-153, Feb. 2001.

[37] I. Kamwa, R. Grondin, D. Asber, J. P. Gingras, and G. Trudel, "Large-scale active load modulation for angle stability improvement," *IEEE Trans. Power Syst.*, vol. 14, no. 2, pp. 582-590, May 1999.

[38] N. D. Huy, L. Dessaint, A. F. Okou, and I. Kamwa, "Selection of input/output signals for wide area control loops," in *Proc. of PES General Meeting*, pp. 1-17, June. 2010.

[39] G. Rogers, *Power System Oscillations*. Norwell, MA: Kluwer, 2000.

[40] B. Pal and B. Chaudhuri, *Robust Control in Power Systems*. New York: Springer-Verlag, 2005.

Biographies

Wei Yao (M'13) received the B.Sc. and Ph.D. degrees in electrical engineering from Huazhong University of Science and Technology (HUST), China, in 2004 and 2010, respectively. Subsequently, he worked as a Postdoctoral Researcher in Department of Electrical Engineering, HUST, from 2010 to 2012. Currently, he is a Lecturer in the College of Electrical and Electronics Engineering, HUST. From October 2012, he also works as a Postdoctoral Research Associate in the Department of Electrical Engineering and Electronics, The University of Liverpool, UK. His research interests include power system stability analysis and control, renewable energy.

L. Jiang (M'00) received the B.Sc. and M.Sc. degrees from Huazhong University of Science and Technology (HUST), China, in 1992 and 1996; and the Ph.D. degree from the University of Liverpool, UK, in 2001, all in Electrical Engineering. He worked as Postdoctoral Research Assistant in the University of Liverpool from 2001 to 2003, and Postdoctoral Research Associate in the Department of Automatic Control and Systems Engineering, the University of Sheffield from 2003 to 2005. He was a Senior Lecturer at the University of Glamorgan from 2005 to 2007 and moved to the University of Liverpool at 2007. Currently, he is a Senior Lecturer in The University of Liverpool. His current research interests include control and analysis of power system, smart grid and renewable energy.

Jinyu Wen (M'10) received the B.Sc. and Ph.D. degrees in electrical engineering from Huazhong University of Science and Technology (HUST),Wuhan, China, in 2004 and 2010, respectively. He was a Post-Doctoral received the B.Sc. and Ph.D. degrees in electrical engineering from Huazhong University of Science and Technology (HUST), Wuhan, China, in 1992 and 1998, respectively. He is a Professor at HUST. He was a Postdoctoral Researcher with HUST from 1998 to 2000, and the Director of Electrical Grid Control Division, XJ Relay Research Institute, Xuchang, China, from 2000 to 2002. His research interests include evolutionary computation, intelligent control, power system automation, power electronics and energy storage.

Q. H. Wu (M'91-SM'97-F'11) received the M.Sc. degree in electrical engineering from Huazhong University of Science and Technology (HUST), China, in 1981; and the Ph.D. degree in electrical engineering from The Queen's University of Belfast (QUB), UK, in 1987. He has been

the Chair of Electrical Engineering in the Department of Electrical Engineering and Electronics, The University of Liverpool since September 1995. His current research interests are advanced control techniques, computational intelligence, and power and energy systems.

Shijie Cheng (M'86-SM'87-F'11) graduated from the Xi'an Jiaotong University, Xi'an, China in 1967 and received a Master of Engineering Degree from the Huazhong University of Science and Technology(HUST), Wuhan, China in 1981 and a Ph.D. from the University of Calgary, Calgary, Canada in 1986 all in the Electrical Engineering. He has been a Professor at the HUST since 1991. His research interests are power system control, stability analysis, application of Artificial Intelligence, and energy storage. Professor Cheng was elected as Fellow of Chinese Academy of Sciences in 2007.